Revisiting the image source model: Towards geometry-based modeling of agent-to-agent channels

Josef Kulmer and Klaus Witrisal
Graz University of Technology, Austria
email: {kulmer, witrisal}@tugraz.at

***Abstract*—This work treats the geometric relationship in multipath propagation of radio-frequency or acoustic channels, used for localizing unknown target nodes. We revisit the image source model and derive a geometric relationship between target nodes and surrounding reflective objects. The obtained relationship reveals insights in the interaction between nodes and reflectors and their impact on estimating multipath parameters. We demonstrate the applicability of the geometric relationship to track nodes without the need of an external infrastructure, e.g. fixed anchor nodes.**

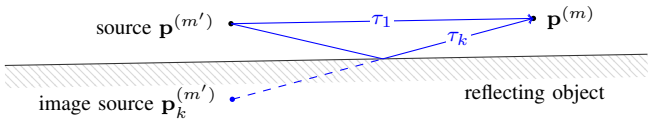

Fig. 1. Application of image source model. The transmitting node m' at position $\mathbf{p}^{(m')}$ (source) is mirrored at the reflecting object to model the specular reflection, received by node m at $\mathbf{p}^{(m)}$.

I. Introduction

Multipath propagation is inherent in channel measurements between any two nodes and serves as a valuable source of position related-information for localization. The works presented in [1], [2], [3], [4], [5], [6], [7] make explicit use of multipath propagation to improve both accuracy and robustness of the localization of target nodes. To exploit the position-related information in multipath components (MPCs) these methods model the measured MPC delays by a geometric relationship of the positions of the nodes as well as the locations of the reflective objects.

To exploit the position-related information in the MPC delays the aforementioned methods apply an image source model [8], [9]. The image source model conceives each multipath as an emitted signal from an image source. It requires the distinction between transmitting (source) node m' and receiving node m where the position of the transmitting node $\mathbf{p}^{(m')} \in \mathbb{R}^2$ is *mirrored* at each reflecting object, resulting in image sources $\left\{\mathbf{p}_k^{(m')}\right\}$, as illustrated in Figure 1. Then the multipath in the received signal at $\mathbf{p}^{(m)} \in \mathbb{R}^2$ can be modeled as direct line to the image sources and subsequently the kth MPC delay τ_k results as geometric distance between the image source $\mathbf{p}_k^{(m')}$ and the receiver. Finally, we obtain a bunch of equations $\left\{\tau_k = \left\|\mathbf{p}_k^{(m')} - \mathbf{p}^{(m)}\right\|/c\right\}$ with $\|\cdot\|$ and c as Euclidean norm and speed of light, which are used to estimate the position $\mathbf{p}^{(m)}$ of node m from a set of delays $\{\tau_k\}$.

The benefits of the image source model are diverse. Considering the case that one of the interacting nodes' position is known (i.e. m') and static [1], [2], [3], [4], [5] then its image source positions can be calculated beforehand. The remaining node m utilizes the image sources to calculate both MPC delays and angles of arrival in order to find its absolute position. In cooperative localization [7] we are interested in estimating both nodes' positions simultaneously. Therefore we require the MPC delays as well as the departing and arriving MPC angles. As the image source model is only capable to formulate the arrival angle, in [7] we calculated the image sources of both interacting nodes in order to obtain both angles. Hereby, each MPC is described by two image sources simultaneously. Node m utilizes the image sources of m' and node m' utilizes the image sources of m. The multipath propagation between both nodes is described by independent image sources which brings us to the major limitation of the image source model. The image sources are not coupled to the original source or reflecting objects and thus, all MPCs are modeled as independent signals. The assumption of independence requires that the MPC delays are not related to each other. As soon as we incorporate higher-order reflections it can easily be shown that the MPC parameters are correlated. Figure 2 illustrates the single reflection k_1 and the double reflection k_2. According to the image source model, the MPCs are independent although both are reflected at object s_1. Any error in the object's location is reflected in the MPC delays and the assumption of independence is violated.

In the following, we revisit the derivation of the image source model. We aim at relating the MPC delays to the location of reflective objects rather than to static image sources. Therefore we can explicitly model the correlations of the MPC parameters as well as the geometric relationship between the interacting nodes and the reflective objects. In Section III we analyze the derived relationship regarding the sensitivity to the reflecting objects' locations and in Section IV we employ the relationship for tracking positions of a cooperative sensor network using information from multipath propagation only.

II. Revisiting the Image Source Model

We consider two nodes m and m' and look at a specific MPC k. For the derivation we distinguish between the transmitting node m' and receiving node m. To model the kth path we introduce the vector $\mathbf{s}_k$ which contains the indices of the reflected objects of the wave traveling from m' to m (the ith reflected object is stored in $[\mathbf{s}_k]_i$ as illustrated in Fig. 2 where $\mathbf{s}_{k_2} = [s_2, s_1]$). Each reflective object s is represented by one point on its surface $\mathbf{p}_s \in \mathbb{R}^2$ and a unit vector $\mathbf{e}_s \in \mathbb{R}^2$ which denotes the object's orientation. Then, after writing the image sources of m' as function of reflective objects and the position of m', the delay of MPC k can be calculated as

$$\tau_k = \|\mathbf{d}\|/c \tag{1}$$

with shorthand

$$\mathbf{d} = \mathbf{p}^{(m)} - \Big(\prod_i \mathbf{A}_{[\mathbf{s}_k]_i}\Big)\mathbf{p}^{(m')} - \sum_i \Big(\prod_{j=i+1} \mathbf{A}_{[\mathbf{s}_k]_j}\Big)\mathbf{b}_{[\mathbf{s}_k]_i}. \tag{2}$$

Here, the first and second term on the right-hand-side are linear functions regarding the sensor nodes' positions. The second term describes the mirroring operation applied on m', also known as *Householder transformation* with Householder matrix $\mathbf{A}_{[\mathbf{s}_k]_i} = (\mathbf{I} - 2\mathring{\mathbf{e}}_{[\mathbf{s}_k]_i}\mathring{\mathbf{e}}_{[\mathbf{s}_k]_i}^{\mathrm{T}})$ and $\mathring{\mathbf{e}}_{[\mathbf{s}_k]_i}$ as counter clockwise, orthogonal unit vector to $\mathbf{e}_{[\mathbf{s}_k]_i}$. The Householder matrix has eigenvalues of ± 1, whereas the eigenvalue of 1 is in the direction of $\mathbf{e}_{[\mathbf{s}_k]_i}$ and the eigenvalue of -1 is along $\mathring{\mathbf{e}}_{[\mathbf{s}_k]_i}$ such that a multiplication with $\mathbf{A}_{[\mathbf{s}_k]_i}$ flips the sign of the coordinate in the direction of $\mathring{\mathbf{e}}_{[\mathbf{s}_k]_i}$ (resulting in the mirroring). The third term is an offset which depends solely on the locations of the reflective objects with $\mathbf{b}_{[\mathbf{s}_k]_i} = 2\mathring{\mathbf{e}}_{[\mathbf{s}_k]_i}\mathring{\mathbf{e}}_{[\mathbf{s}_k]_i}^{\mathrm{T}}\mathbf{p}_{[\mathbf{s}_k]_i}$. The offset attains zero if the origin of coordinates is located on the reflective objects (i.e. there exists a $\mathbf{p}_{[\mathbf{s}_k]_i} = \mathbf{0}$).

It is interesting to note, that (2) can be rewritten such that transmitter and receiver change their role by reversing the chronological order of the reflected objects in $\mathbf{s}_k$. Therefore, it can be used to calculate the MPC delay as well as the departing and arrival MPC angle using the same equation. In the concept of image sources, one can only calculate the arrival angles; to obtain departing angles the calculation of image sources needs to be repeated from the receiving node's view.

III. Insights

The derived geometric relationship presents valuable insights how the MPC delay is influenced by the node positions and orientation of the reflective objects. We calculate the partial derivative of (1) to make the impact of the geometric relationship on the MPC delays more visible. It illustrates how a displacement of $\mathbf{p}^{(m)}$, $\mathbf{p}^{(m')}$ and $\{\mathbf{p}_s\}$ affects τ_k.

The derivatives with respect to both node positions follow as

$$\frac{\partial \tau_k}{\partial \mathbf{p}^{(m)}} = \frac{\mathbf{d}}{c\|\mathbf{d}\|}, \quad \frac{\partial \tau_k}{\partial \mathbf{p}^{(m')}} = \frac{\mathbf{\Psi}\mathbf{d}}{c\|\mathbf{d}\|}$$

where $\mathbf{d}/\|\mathbf{d}\|$ is the normalized direction of the arriving MPC and the multiplication by $\mathbf{\Psi} = -\prod_i \mathbf{A}_{[\mathbf{s}_k]_i}$ accounts for the geometric relationship to the reflectors by redirecting the departing MPC. It can be shown that both derivatives with respect to the sensor nodes attain a slope with absolute value of $1/c$ ($\|\partial\tau_k/\partial\mathbf{p}^{(m)}\| = \|\partial\tau_k/\partial\mathbf{p}^{(m')}\| = 1/c$) and pointing in the direction of the arriving / departing MPC.

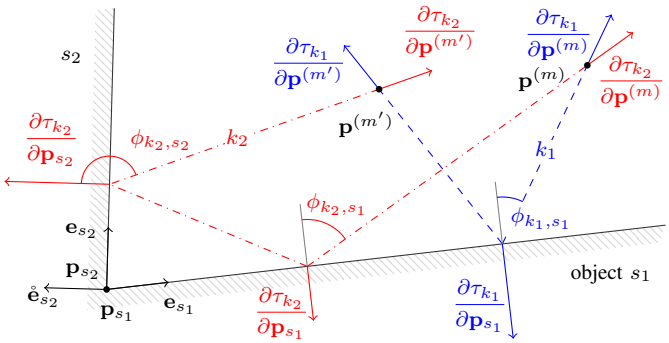

Fig. 2. Illustration of a single (k_1) and double reflection (k_2). The partial derivatives (arrows) exemplify the delay sensitivity regarding the positions of nodes and reflecting objects. MPC k_2 is reflected at both s_1 and s_2 whereas its delay τ_{k_2} is more affected by s_2 justified by the steeper MPC angle ϕ_{k_2,s_2} at the reflection point (comparing the length of the derivatives).

The derivative with respect to the ith reflective object location is equivalent to

$$\frac{\partial \tau_k}{\partial \mathbf{p}_{[\mathbf{s}_k]_i}} = -2\frac{\cos(\phi_{k,[\mathbf{s}_k]_i})\mathring{\mathbf{e}}_{[\mathbf{s}_k]_i}}{c}$$

with $\phi_{k,[\mathbf{s}_k]_i}$ as angle between arriving / departing MPC and object orientation $\mathring{\mathbf{e}}_{[\mathbf{s}_k]_i}$. It is interesting to note that the gradient points away from the nodes along the direction of $\pm\mathring{\mathbf{e}}_{[\mathbf{s}_k]_i}$. Furthermore, the delay is more sensitive for objects with steeply arriving MPCs (compare ϕ_{k_2,s_1} with ϕ_{k_2,s_2} in Figure 2). An arriving angle at the reflection point of $\phi = 0°$ yields a doubled sensitivity of τ_k to the reflecting object location compared to the sensor node position: $\|\partial\tau_k/\partial\mathbf{p}_{[\mathbf{s}_k]_i}\| = 2\|\partial\tau_k/\partial\mathbf{p}^{(m)}\| = 2/c$.

IV. Application

In the following we employ the derived relationship between positions of nodes and locations of reflective objects for anchor-free tracking of sensor nodes using real data. Knowledge of reflective objects enables the association of MPCs to the surrounding geometry which compensates for the demand of anchor nodes with known positions. In our setup we consider four nodes moving on trajectories of $n \in \{1, \ldots, 200\}$ steps in a hallway, as illustrated in Figure 3. At each time step n the nodes perform channel measurements where we distinguish between *self* and *relative* measurements. At self measurements a single node explores the reflections from the surrounding environment. For these measurements we equipped each node with two antennas, assembled next to each other. The measured channel response between both antennas contains reflections only (as the line-of-sight (LOS) component arrives at $\tau_{\mathrm{LOS}} \approx 0$). The relative measurements are performed between neighboring nodes, and we obtain in total four self and six relative measurements at each n.

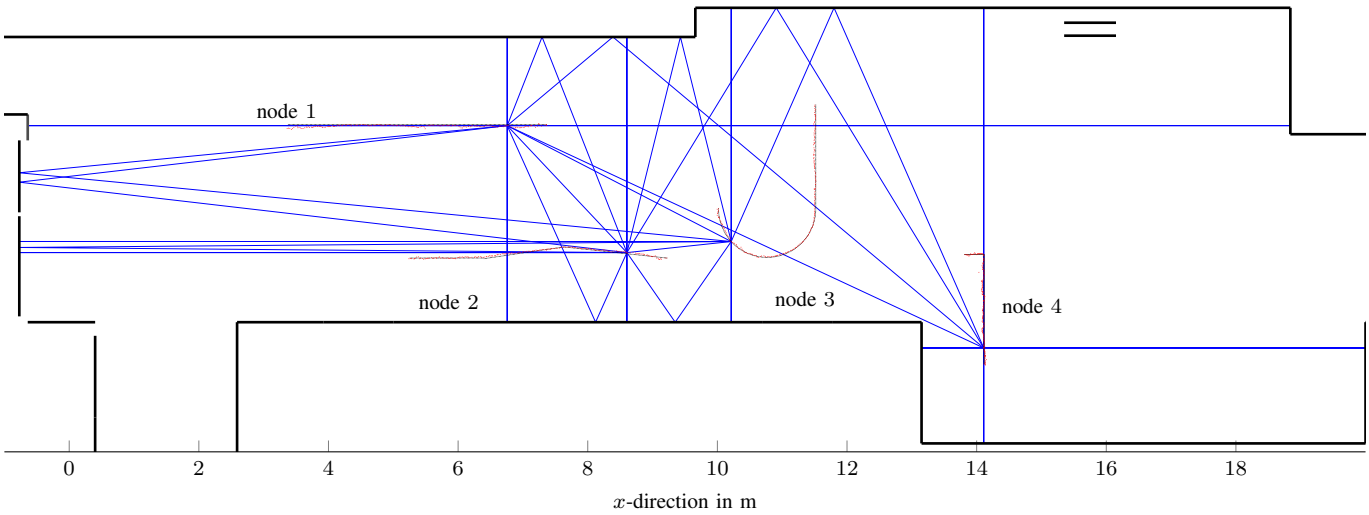

Fig. 3. Illustration of the hallway and the trajectories of the nodes. Black and red crosses are the true and estimated nodes' positions. The multipath propagation at time step $n = 30$ is shown in blue.

We performed the channel measurements using a correlative channel sounder where we convolved the received impulse response with a raised cosine pulse with pulse duration of 1 ns (which corresponds to a 3 dB bandwidth of 1 GHz), roll off factor of 0.5 and carrier frequency of 7 GHz. The MPC delays of each measurement are estimated using [1].

To model the floorplan we considered objects with dimension greater than 25 cm, e.g. walls, doors and windows. The floorplan parameters $\{\mathbf{p}_s\}$ and $\{\mathbf{e}_s\}$ were obtained using a measuring tape. Note, the required floorplan accuracy depends on the transmitted signal. Large bandwidths of 1 GHz enable ranging in cm range [10]. Hence, accurate floorplans are required for an unbiased modeling of the MPC delays (see [7] for an experimental evaluation of the floorplan's impact).

We employ an Extended Kalman Filter to recursively estimate the nodes' positions using the measured MPC delay information. As measurement model we use the derived relationship in (1) where we consider that at self measurements the transmitting and receiving node in (1) attains the same position. At each time step the nodes' positions (red crosses in Figure 3) are jointly estimated using the linearized measurement model which is equivalent to the partial derivatives of (1), derived in Section III.

Figure 4 shows the cumulative distribution function of the position error. We can observe that the nodes are able to estimate their positions with high accuracy using information contained in multipath only. The 90 % limit of the position errors is below 6 cm which justifies the eligibility of the derived geometric relationship. It is interesting to note that the performance of nodes 2 and 3 is slightly better compared to nodes 1 and 4. This can be reasoned as nodes 2 and 3 are well surrounded by cooperative neighboring nodes. Thus, it is more likely to receive multipaths from uniformly distributed directions which subsequently reduces the position error in both dimensions. This is different at nodes 1 and 4 whose positions are separated from the neighboring nodes (see Figure 3). Their position related information is obtained from mainly one direction which limits the achieved accuracy in the perpendicular direction.

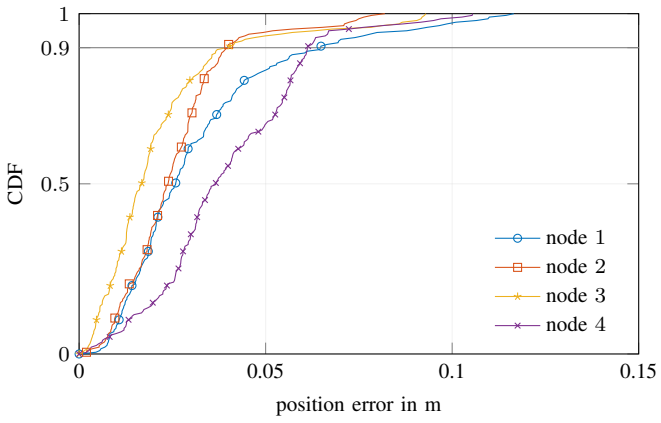

Fig. 4. Cumulative distribution function of the position error of nodes $1-4$.

V. Conclusion

We revisited the image source model for assessing the impact of node positions and reflecting object locations on the multipath propagation. We pointed out that the MPC delays are more sensitive to errors in the reflecting object locations (up to a factor of 2) compared to the sensor node positions. Our findings support the importance of highly accurate locations of the reflecting objects due to their strong impact on the MPC delays. We demonstrated the benefits of the derived geometric relationship by tracking the positions of cooperative nodes using multipath propagation only. Future work will expand the investigations to point scatters and complex shapes of reflectors.

REFERENCES

[1] P. Meissner and K. Witrisal, "Analysis of Position-Related Information in Measured UWB Indoor Channels," in *6th European Conference on Antennas and Propagation (EuCAP)*, 2012.

[2] R. Parhizkar, I. Dokmanic, and M. Vetterli, "Single-channel indoor microphone localization," in *2014 IEEE International Conference on Acoustics, Speech and Signal Processing (ICASSP)*, May 2014.

[3] E. Tsalolikhin, I. Bilik, and N. Blaunstein, "A single-base-station localization approach using a statistical model of the NLOS propagation conditions in urban terrain," *IEEE Transactions on Vehicular Technology*, vol. 60, no. 3, pp. 1124–1137, 2011.

[4] W. Xu, F. Quitin, M. Leng, W. P. Tay, and S. G. Razul, "Distributed localization of a RF target in NLOS environments," *IEEE Journal on Selected Areas in Communications*, vol. 33, no. 7, July 2015.

[5] Y. Shen and M. Win, "On the Use of Multipath Geometry for Wideband Cooperative Localization," in *IEEE Global Telecommunications Conference (GLOBECOM)*, 2009.

[6] H. Naseri, M. Costa, and V. Koivunen, "Multipath-aided cooperative network localization using convex optimization," in *2014 48th Asilomar Conference on Signals, Systems and Computers*, Nov 2014.

[7] J. Kulmer, E. Leitinger, P. Meissner, S. Hinteregger, and K. Witrisal, "Cooperative localization and tracking using multipath channel information," in *2016 International Conference on Localization and GNSS (ICL-GNSS)*, June 2016, pp. 1–6.

[8] J. Borish, "Extension of the image model to arbitrary polyhedra," *The Journal of the Acoustical Society of America*, vol. 75, no. 6, 1984.

[9] J. B. Allen and D. A. Berkley, "Image method for efficiently simulating small-room acoustics," *The Journal of the Acoustical Society of America*, vol. 65, no. 4, pp. 943–950, 1979.

[10] J. Kulmer, S. Hinteregger, B. Growindhager, M. Rath, M. S. Bakr, E. Leitinger, and K. Witrisal, "Using DecaWave UWB transceivers for high-accuracy multipath-assisted indoor positioning," in *2017 IEEE International Conference on Communications Workshops (ICC Workshops)*, May 2017, pp. 1239–1245.